scientific reports

Check for updates

OPEN

# YKL-40 inhibits melanoma progression and metastasis by inducing immune cell infiltration in a mouse model

Hailong Zhang[1,2,4], Xiangyu Zhao[1,4], Mengqi Shi[1,3], Yuqi Han[1], Kun Lu[1], Hongyu Wang[1], Sipeng Sun[1,2], Ben Yang[1,2], Zhiqin Gao[1], Meihua Qu[2], Guohui Wang[1], Yi Wang[1], Wenjing Yu[1]✉ & Yubing Wang[1,2]✉

**YKL-40 is a glycoprotein that has been extensively studied due to its elevated expression in numerous solid tumors, and its expression is altered in melanoma, where its levels in tumor tissues are notably lower compared with those in normal skin tissues. Patients with melanoma exhibiting high YKL-40 expression have improved survival rates, suggesting a potential tumor-suppressive function of YKL-40 in melanoma. The present investigation into the ectopic expression of YKL-40 in human (A375) and murine (B16F10) melanoma cell lines demonstrated a consequential decrease in cell proliferation, migration and invasion. Furthermore, YKL-40 overexpression was associated with suppressed tumor growth in a subcutaneous melanoma mouse model and diminished tumor cell metastasis in a pulmonary metastasis model. RNA-sequencing analysis revealed that YKL-40 overexpression led to the upregulation of immune cell infiltration-related signaling pathways, including cytokine receptor interactions, natural killer cell-mediated cytotoxicity, and T and B lymphocyte receptor signaling. These findings highlight the potential of YKL-40 as a regulator of tumor-immune interactions in melanoma, highlighting its prospective utility in immunotherapy-based treatment strategies for melanoma.**

**Keywords** Chitinase 3 like 1, Melanoma, Immune cell, Infiltration, Transcriptomes

Melanoma is a highly malignant tumor that arises from the malignant transformation of melanocytes, pigment-producing cells of neural crest origin, primarily located in the skin. It is characterized by a high propensity for metastatic invasion and is one of the leading causes of death associated with skin malignancies[1,2]. According to the latest statistics from the American Cancer Society, it is estimated that in 2025, about 104,960 new melanomas will be diagnosed in the United States, and approximately 8,430 people will die from the disease. Traditional melanoma treatments, including surgery, radiation therapy and chemotherapy, are often ineffective due to resistance of tumors, leading to poor prognostic outcomes and high mortality rates[3]. Prior to the advent of immunotherapy, the therapeutic landscape was dominated by chemotherapeutic agents such as dacarbazine, temozolomide and flutemustine, which seldom met expectations in prolonging survival or enhancing the quality of life of patients[4]. Although immunotherapy and targeted therapies have improved survival metrics, the benefits are often transient, necessitating further research and therapeutic advancements[5]. It has been revealed that melanoma is a highly immunogenic tumor, and the depleted immune response of the body is an important cause of tumor development and metastasis, thus immunotherapy against melanoma has received widespread attention[6]. Owing to advancements in treatment, the rate of 5-year survival for patients with advanced melanoma has significantly increased from approximately 10% in the dacarbazine era to about 50%[7]. Immune cell infiltration in melanoma plays a crucial role in tumor progression and response to therapy. Cytotoxic T cells (CD8 + T cells) are often present within the tumor microenvironment, and a higher density of these cells is typically associated with better patient outcomes; however, melanoma can evade T cell-mediated destruction by upregulating inhibitory

[1]School of Life Science and Technology, Shandong Second Medical University, 7166 Baotong Street, Weifang 261053, Shandong, People's Republic of China. [2]Translational Medical Center, The No.2 People's Hospital of Weifang, Weifang 261041, Shandong, People's Republic of China. [3]Center for Translational Medicine, Baotou Medical College, Baotou 014040, Inner Mongolia, People's Republic of China. [4]Hailong Zhang and Xiangyu Zhao contributed equally to this work. ✉email: yuwjwf@163.com; ybwang@link.cuhk.edu.hk

checkpoints like PD-L1[8,9]. Conversely, regulatory T cells (Tregs), which are enriched in melanoma tumors, can suppress anti-tumor immune responses and correlate with poorer clinical outcome[10]. Myeloid cells, particularly tumor-associated macrophages (TAMs), tend to exhibit a pro-tumorigenic phenotype, secreting factors that promote tumor growth and angiogenesis while also suppressing T cell activity[11]. Dendritic cells (DCs) can initiate immune responses, but their function may be impaired in the melanoma microenvironment[12]. Natural killer (NK) cells, part of the innate immune response, can directly kill melanoma cells, but their activity is often hindered by immunosuppressive factors secreted by tumor cells[13]. The melanoma microenvironment is also characterized by various cytokines and chemokines that recruit immune cells; for example, CCL2 and CXCL10 are involved in attracting T cells and monocytes to the tumor site[14]. Overall, the dynamics of immune cell infiltration in melanoma illustrate a complex interplay where immune cells can both suppress and promote tumor growth, highlighting the need for targeted immunotherapeutic strategies.

Chitinase 3 like 1 (YKL-40), a protein encoded by the CHI3L1 gene, was originally identified in mouse breast cancer cells, is named after its three N-terminal amino acid residues of tyrosine, lysine and leucine and its molecular mass of 40 kDa, and is highly homologous to chitinase[15]. YKL-40 is predominantly secreted by macrophages, neutrophils and cancer cells under the regulation of cytokines such as IL-13, IL-6, IL-1β and IFN-γ[16]. Elevated YKL-40 expression has been observed in various solid tumors, where it contributes to processes such as cell proliferation, angiogenesis, inflammation, extracellular matrix remodeling and inhibition of apoptosis[17–20]. Furthermore, YKL-40 has been suggested to promote invasion and metastasis via epithelial-mesenchymal transition in several cancer types[21,22]. Therefore, YKL-40 has served as a potential target for cancer treatment in numerous studies[23–25].

It has been demonstrated that application of anti-YKL-40 monoclonal antibodies reduced tumor growth in a mouse transplantation tumor model of human glioblastoma and lung cancer[26,27]. However, melanoma exhibits a divergent response, with targeting of YKL-40 leading to an increased tumor volume in xenograft models[28]. The present investigation of the role of YKL-40 in melanoma revealed its potential tumor-suppressive effects, mediated via enhanced immune cell infiltration. The present study elucidated the multifaceted role of YKL-40 in melanoma and suggested its prospective inclusion in immunotherapy-based treatment regimens.

## Materials and methods

### Cell lines and culture

Cell lines, including HEK293T, A375, A875 and B16F10 cell lines, were purchased from Cell Resource Center (Institute of Basic Medical Sciences, Peking Union Medical College). All cells were cultured in DMEM (cat. no. SH30081.LS; HyClone; Cytiva) supplemented with 10% FBS (cat. no. FSP500; Shanghai ExCell Biology, Inc.) and penicillin/streptomycin (100 mg/ml; cat. no. 15140122; Gibco; Thermo Fisher Scientific, Inc.) at 37 °C in a 5% $CO_2$ incubator.

For transfection and creation of stable cell lines, the pBabe-puro empty vector and YKL-40-containing vector plasmids were extracted according to the instructions of the plasmid extraction kit (cat. no. DP117; Tiangen Biotech Co., Ltd.). HEK293T cells were transfected with pBabe and packaging vector pCL-Ampho using the liposome transfection method (Lipofectamine 2000; cat. no. 11668019; Invitrogen; Thermo Fisher Scientific, Inc.). Viral supernatant was collected after 72 h, centrifuged and added to the target cells at a 3:4 ratio with DMEM complete medium. After 24 h, the medium was replaced with medium containing puromycin (0.5 μg/ml; cat. no. HY-K1057; MedChemExpress) for positive clone screening.

### Cell lysis and immunoblotting

Cellular protein lysates were extracted using RIPA buffer (50 mM Tris-HCl pH 7.5, 1% Triton X-100, 150 mM NaCl, 10 mM $MgCl_2$, 0.1% SDS, 0.5% sodium deoxycholate and protease inhibitor cocktail). The total protein concentration was determined using a BCA protein assay kit (cat. no. 23225; Thermo Fisher Scientific, Inc.). Cell lysates were mixed with 5X Laemmli sample buffer, boiled for 4 min at 95 °C and then stored at -20 °C. Equal amounts of total protein were resolved by 10% SDS-polyacrylamide gel electrophoresis and transferred to a nitrocellulose membrane. The membranes were blocked with 5% skim milk in Tris-buffered saline containing 0.1% Tween for 1 h at room temperature, and incubated with the appropriate primary and secondary antibodies. Labeled proteins were visualized using ECL western blotting detection reagents. The antibodies used for immunoblotting were: YKL-40 (cat. no. 47066; Cell Signaling Technology, Inc.), β-actin (cat. no. 4967 S; Cell Signaling Technology, Inc.) and anti-rabbit HRP-conjugated secondary antibody (cat. no. 7074 S; Cell Signaling Technology, Inc.).

### Cell viability assay

Cell viability was examined using an MTS assay kit (Promega Corporation). For viability assays, cells ($1 \times 10^4$) were plated in 96-well plates and allowed to adhere overnight. After 24 h of seeding, cells were treated with doxorubicin (cat. no. HY-15142 A; MedChemExpress), cisplatin (cat. no. MB1055; Dalian Meilun Biology Technology Co., Ltd.) and temozolomide (cat. no. HY-17364; MedChemExpress) for 72 h. Following treatment, the medium was removed from the wells. PMS (Phenazine Methosulfate), MTS and DMEM colorless medium were mixed at a ratio of 1:20:100 to prepare MTS working solution. Subsequently, 100 μl MTS working solution was added to each well, cells were incubated for 10 min at 37 °C, the absorbance at 490 nm was measured using a plate reader.

### Colony formation assays

Cells were cultured in DMEM containing 10% FBS, penicillin (100 units/ml) and streptomycin (100 ng/ml) in a 5% $CO_2$ incubator at 37 °C. The medium was replaced every 3 days. After 14 days, colonies were stained with Crystal Violet and counted.

### Cell migration assays

For the wound healing assay, cells were seeded in 6-well plates and cultured at 37 °C overnight until a confluent monolayer was formed. Subsequently, a wound was created by manually scratching the monolayer using a sterile 200-µl pipette tip. The wounded monolayer was then washed three times with PBS to remove cell debris and incubated with fresh medium containing 1% FBS. Images of the scratched area were captured at 0, 20 and 24 h after scratching. The wound closure efficacy was quantified by calculating the percentage of area healed by the cells relative to the initial wound area.

### Cell invasion assays

For the invasion assay, a total of $1 \times 10^6$ cells in 300 µl of 1% FBS medium were added to the Matrigel-coated upper chamber, and 700 µl of 10% FBS medium was added to the lower chamber. After incubation in a humidified tissue culture incubator for 36 h, the noninvasive cells on the upper surface of the membrane were gently removed with a cotton swab. The invading cells that had traversed to the lower surface of the membrane were fixed in paraformaldehyde for 10 min, treated with 0.2% Triton for 10 min to increase cell membrane permeability, stained with DAPI for 10 min and rinsed three times with PBS. Cell counting was carried out by capturing images of the membrane with a fluorescence microscope. Images of five random fields of view were captured under the fluorescence microscope to quantify the invading cells.

### Mouse tumor models

Male C57BL/6 mice were obtained from and maintained in the Animal Holding Center of Weifang Medical University (Shandong Second Medical University). Mice (6 weeks) were subcutaneously implanted with cells ($5 \times 10^5$ cells in 200 µl saline) in the lateral aspect of the left hind leg. Tumor volumes were assessed every alternate day commencing on day 13 post-inoculation, and mice were sacrificed by intraperitoneal injection of sodium pentobarbital (150 mg/kg). on day 19. After dissecting the mice, the tumors were weighed and the volume was measured. Half of the tumors were fixed in tissue fixative, while the other half were frozen for transcriptome sequencing analysis. The tumor volume was calculated using the following formula: Tumor volume ($mm^3$) = 0.5 x [width (mm)] $^2$ x [length (mm)].

For lung metastasis analysis, female C57BL/6J mice (6 weeks) were intravenously injected with $4 \times 10^5$ cells in 500 µl saline into the lateral tail vein. At 15 days post-inoculation, the mice were sacrificed by intraperitoneal injection of sodium pentobarbital (150 mg/kg) and subjected to dissection, during which all organs were visually inspected for the existence of macroscopic melanoma metastases. Metastatic nodules were counted under a dissecting microscope.

All animal experiments were performed in accordance with the guidelines and regulations of the Ministry of Science and Technology of China. The protocol was approved by the Ethics Committee of Weifang No.2 People's Hospital (approval no. 2024LAC019). All efforts were made to minimize animal suffering and to reduce the number of animals used in the study. The experiments also adhered to the ARRIVE guidelines (https://arriveguidelines.org) to ensure complete and transparent reporting of the methods and results.

### Hematoxylin-eosin and Immunofluorescence staining

The tumor and lung tissues were removed and fixed in 4% paraformaldehyde solution at room temperature for 48 h. Subsequently, the tissues underwent dehydration, paraffin embedding and sectioning. The sections were stained with hematoxylin-eosin dye and subsequently scanned using a pathology section scanner. Nodules present on organs displaying evident melanoma metastases were quantified under a dissecting microscope. For Immunofluorescence staining, sections were permeabilized with 0.1–0.25% Triton X-100 in PBS, blocked with 1% BSA in PBST, and stained with primary antibodies against CD3 (cat. no. A19017; ABconal) and CD68 (cat. no. A15037; ABconal), followed by fluorescent-conjugated secondary antibodies. Nuclei were counterstained with DAPI. After mounting, sections were observed using a fluorescence-microscope.

### Quantitative RNA-sequencing (RNA-seq) and data analysis

The tumor tissues dissected from model mice were lysed in 1 ml TRIzol™ Reagent (cat. no. 15596026; Invitrogen; Thermo Fisher Scientific, Inc.). Total RNA was extracted and analyzed using an Agilent 2100 Bioanalyzer (Agilent Technologies, Inc.). Following RNA qualification, the samples were subjected to quantitative RNA-seq by Shanghai Genesky Biotechnologies, Inc. Differential expressed genes (DEGs) were identified with a threshold set at a $\log_2$ value > 1 and $P < 0.05$. For functional analysis, a gene set enrichment analysis (GSEA; Broad Institute) tool kit was used to obtain the enrichment score for defined gene sets, such as hallmark gene sets, Gene Ontology gene sets and Kyoto Encyclopedia of Genes and Genomes (KEGG) pathway gene sets. The data discussed in the present study have been deposited in the National Center for Biotechnology Information Gene Expression Omnibus database and can be accessed via the Gene Expression Omnibus series accession number GSE217590.

### Statistical analysis

Data are presented as the mean ± SD for the in vitro experiments and the mean ± SEM for the in vivo experiments. Differences in the results of two groups were evaluated using either an unpaired two-tailed Student's t-test or one-way ANOVA followed by Dunnett's post hoc test. $P < 0.05$ was considered to indicate a statistically significant difference.

## Results

### Downregulation of CHI3L1/YKL-40 in melanoma is associated with poor prognosis

Investigation has linked elevated serum/plasma YKL-40 levels to increased mortality in patients with melanoma[29]; however, the source of YKL-40, such as immune cells or the tumor itself, remains uncertain. To examine YKL-

40 expression in melanoma tissues, mRNA levels were analyzed using data from various databases. Notably, CHI3L1/YKL-40 expression was significantly lower in melanoma tumors than in normal skin tissues, as revealed by The Cancer Genome Atlas RNA-seq data Fig. 1A). Consistent findings were observed in the Gene Expression Database of Normal and Tumor Tissues utilizing Human Genome U133 microarrays Fig. 1B,C). Lower CHI3L1/YKL-40 expression was associated with reduced survival in patients with melanoma, suggesting a potential tumor-suppressive role of YKL-40 Fig. 1D). Given the propensity of melanoma for metastasis, analysis of two independent datasets, encompassing gene expression data from normal, tumor and metastatic stages, confirmed the significant reduction of CHI3L1/YKL-40 mRNA levels in both tumor and metastatic tissues compared with normal tissues Fig. 1E,F). This downregulation of gene expression in melanoma may be related to the hypermethylation status in the promoter region of the CHI3L1 gene Fig. 1G).

## YKL-40 overexpression inhibits melanoma cell proliferation, migration and invasion

To explore the biological roles of YKL-40 in melanoma, cell lines overexpressing YKL-40 were established using both human (A375) and murine (B16F10) melanoma cells Fig. 2A). Colony formation assays demonstrated significant proliferation inhibition in A375 cells due to YKL-40 overexpression Fig. 2B,C). A similar trend was observed in B16F10 cells, although it was not statistically significant Fig. 2B,D). Wound healing assays further confirmed the role of YKL-40 in reducing migration in both cell lines Fig. 2E–H). Additionally, Matrigel-coated Transwell assays revealed decreased invasion in B16F10 cells overexpressing YKL-40 Fig. 2I,J). Collectively, these results indicated that YKL-40 overexpression inhibited melanoma cell proliferation, migration and invasion. In addition, drug resistance constitutes one of the difficulties in the clinical treatment of melanoma. Thus, the present study examined whether YKL-40 might increase drug sensitivity in response to chemotherapeutic agents. However, YKL-40 overexpression did not enhance sensitivity to conventional chemotherapeutic agents (temozolomide, cis-platinum and dacarbazine) in A375 cells (Fig. S1A-C).

## YKL-40 suppresses melanoma tumorigenesis and lung metastasis in vivo

A subcutaneous tumor model was established in male C57BL/6 mice using B16F10 cells transfected with either a control vector or a YKL-40 overexpression vector Fig. 3A). Tumors were measurable by day 13 post-transplantation, with volumes recorded every alternate day. On day 19, mice were euthanized, and tumors were

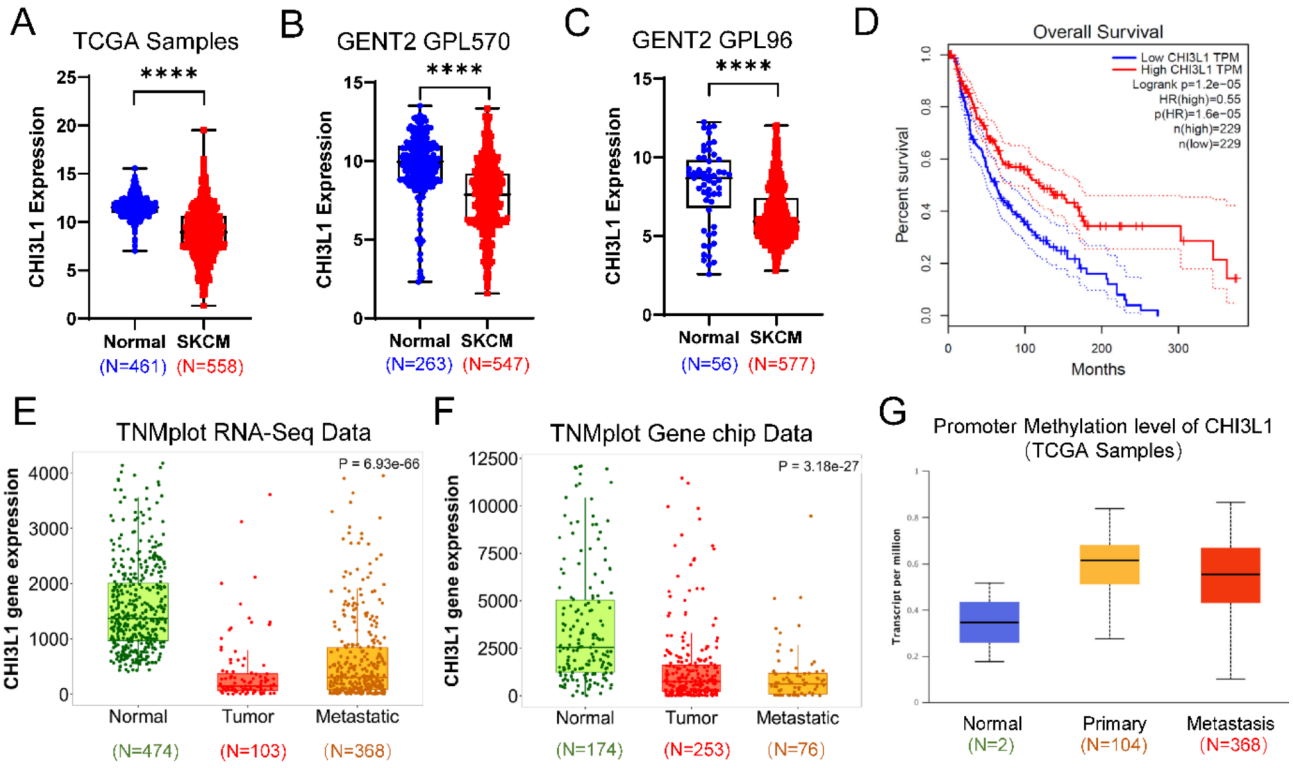


**Fig. 1**. CHI3L1/YKL-40 expression is downregulated in melanoma tumors with poor prognosis. (**A**–**C**) CHI3L1/YKL-40 expression was reduced in melanoma tumors compared with normal skin tissues in The Cancer Genome Atlas RNA-sequencing collections and the Gene Expression Database of Normal and Tumor Tissues database. (**D**) Kaplan-Meier curve of survival probability in patients with melanoma with different expression levels of CHI3L1/YKL-40. Data were adopted from the Gene Expression Profiling Interactive Analysis database. (**E** and **F**) CHI3L1/YKL-40 mRNA levels were reduced in tumor and metastatic tissues compared with normal tissues. Data were obtained from two independent datasets, including normal, tumor and metastatic melanoma data, from TNMplot. (**G**) Hypermethylation in the promoter region of the CHI3L1 gene may downregulate gene expression. YKL-40, chitinase 3 like 1.

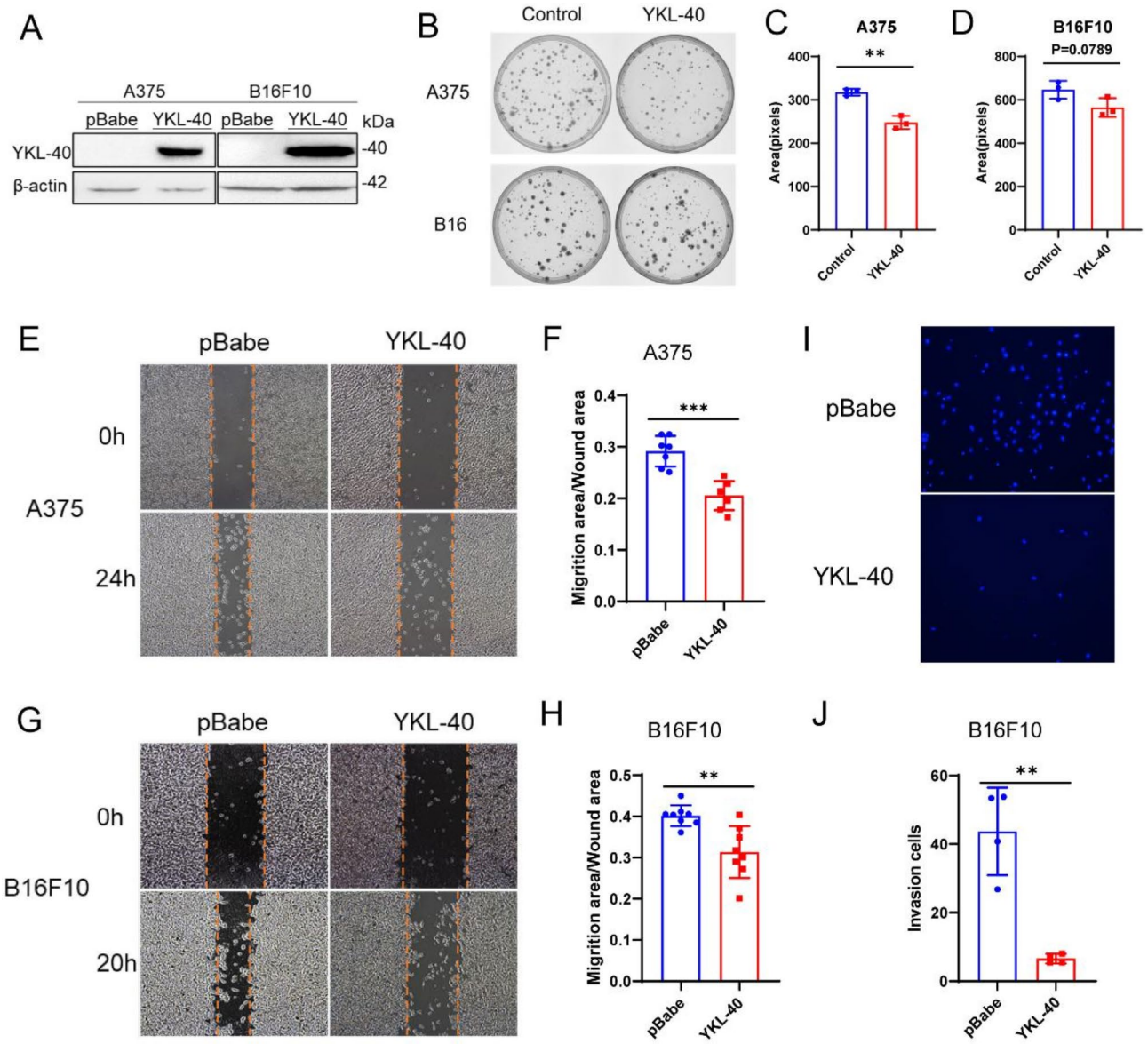


**Fig. 2**. YKL-40 overexpression reduces the malignancy of melanoma cells. (**A**) Melanoma cell lines with stable overexpression of YKL-40 were established using a retroviral transfection method. The expression levels and secretion of YKL-40 were detected by western blotting. pBabe, empty backbone vector. YKL-40, over-expressing vector. Original blots are presented in Supplementary Figure S3. (**B**) A375 and B16F10 cells were seeded in a 60-mm culture dish at a density of 200 cells/plate and cultured for 2 weeks to form colonies. The cell colonies were stained with crystal violet. (**C** and **D**) Colony areas were quantified using Fiji-ImageJ (bars, SD; t-test; $^{**}P<0.01$; $n=3$). (**E** and **G**) Monolayers of A375 or B16F10 cells were scratched with a 200 µl pipette tip when 95% confluence was reached. Representative images of migrating cells were captured under an inverted microscope (magnification, x40). (**F**) The migration of A375 cells was quantified based on the wound closure area 24 h after scratching (migration area / wound gap area; bars, SD; t-test; $^{***}P<0.001$; $n=7$). (**H**) The migration of B16F10 cells was quantified based on the wound closure area 20 h after scratching (migration area / wound gap area; bars, SD; t-test; $^{**}P<0.01$; $n=8$). (**I**) B16F10 cells that migrated to the bottom side of the Transwell chamber were fixed and stained with DAPI. Representative images of migrating cells were captured under an inverted microscope (magnification, x100). (**J**) The number of migrated cells was quantified using Fiji-ImageJ (bars, SD; t-test; $^{**}P<0.01$; $n=4$). YKL-40, chitinase 3 like 1.

excised and weighed Fig. 3B). During the experimental period, it was observed that the body weights of the mice did not show any significant changes Fig. 3C). The tumors from YKL-40-overexpressing cells were significantly smaller Fig. 3D–G), indicating its inhibitory effect on B16F10 cell tumorigenesis. Histological examination revealed less aggressive tumor cell characteristics in the YKL-40 overexpression group compared with the control group Fig. 3H,I).

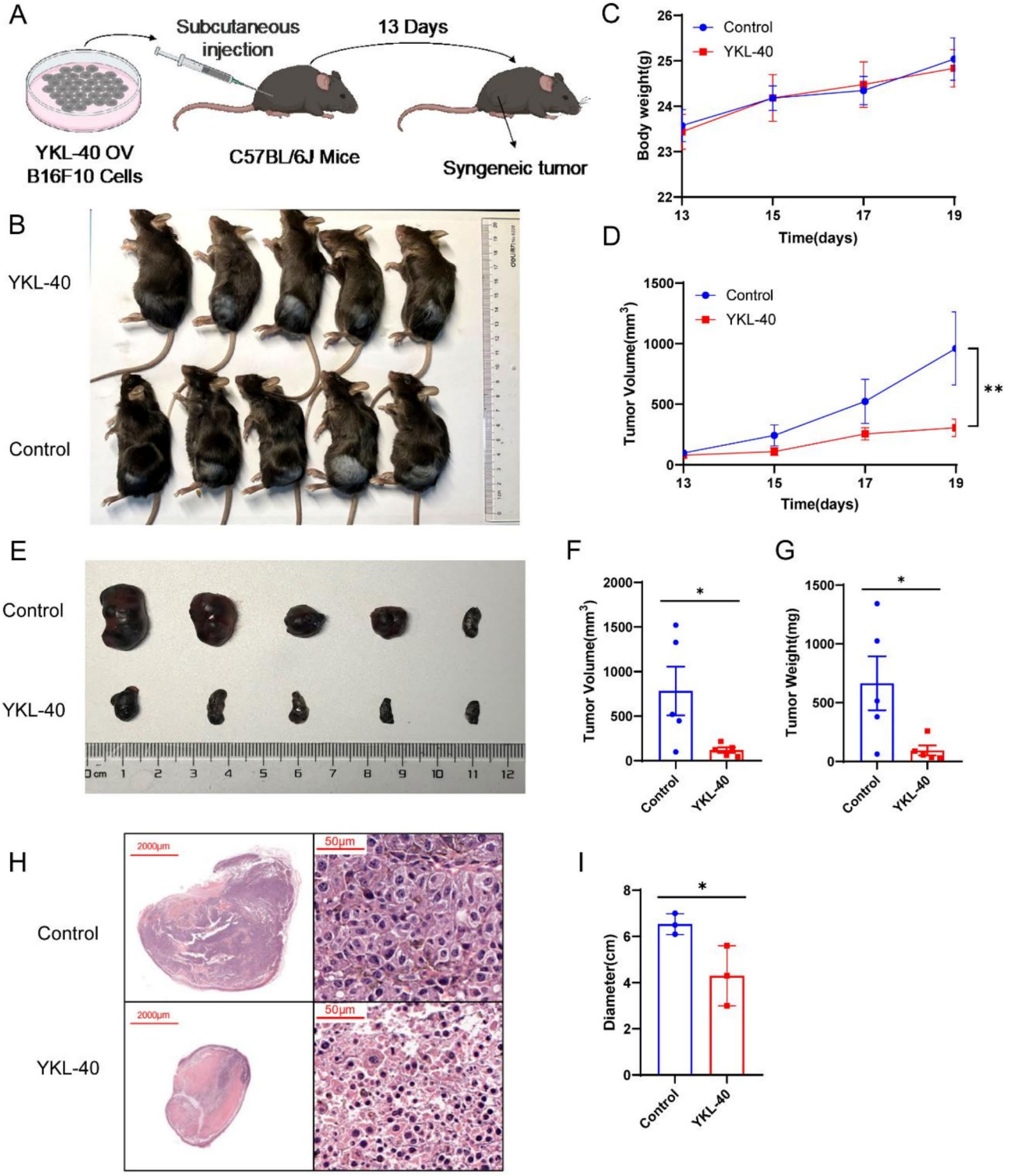


**Fig. 3**. YKL-40 inhibits tumorigenesis of melanoma in vivo. (**A**) Schematic of subcutaneous tumor model in male C57BL/6 mice established via injection with B16F10 cells transfected with either blank vector or YKL-40 overexpression vector. (**B**) Body weight changes in tumor-bearing mice. (**C**) Images of tumor-bearing mice in each group after 13 days. (**D**) Folding line graph of the changes in tumor volume. (**E**) Images of tumors. (**F** and **G**) Histograms of tumor weight and volume (bars, SEM; t-test; $^{*}P < 0.05$; $n = 5$). (**H**) H&E staining of melanoma tumor tissue. (**I**) Histograms of tumor diameters determined by H&E staining (bars, SEM; t-test; $^{*}P < 0.05$; $n = 5$). YKL-40, chitinase 3 like 1.

To further investigate the role of YKL-40 in the metastasis of melanoma cells in vivo, a metastasis assay was performed. Control and YKL-40-overexpressing B16F10 cells were injected into the lateral tail vein of C57BL/6 mice. At 15 days post inoculation, the mice were sacrificed, and all major organs were checked for the generation of tumor metastases (Fig. 4A). Lung metastases were predominantly observed, with a significant reduction in metastatic nodules in mice injected with YKL-40-overexpressing cells (Fig. 4B,C). Histological analysis confirmed fewer and smaller metastatic lesions in the YKL-40 group (Fig. 4D–F), indicating the suppressive effect of YKL-40 on melanoma metastasis.

### RNA-seq analysis revealed that YKL-40 induces immune cell infiltration of melanoma in vivo

To explore the mechanisms of how YKL-40 regulates tumor progression in vivo, transcriptome sequencing analysis of subcutaneous tumor tissues was performed. The threshold for DEGs was set at a fold change > 2 and an adjusted P-value < 0.05. The volcano plot shows 903 upregulated DEGs and 437 downregulated DEGs in the YKL-40 overexpression group Fig. 5A). Gene ontology enrichment analysis revealed that DEGs were primarily involved in immune cell responses, such as T cell activation, chemokine binding and activity, and regulation of immune cell adhesion, which indicated that YKL-40 expression served important roles in the immune cell regulation process (Fig. S2). Similar results were also observed in KEGG enrichment analysis,

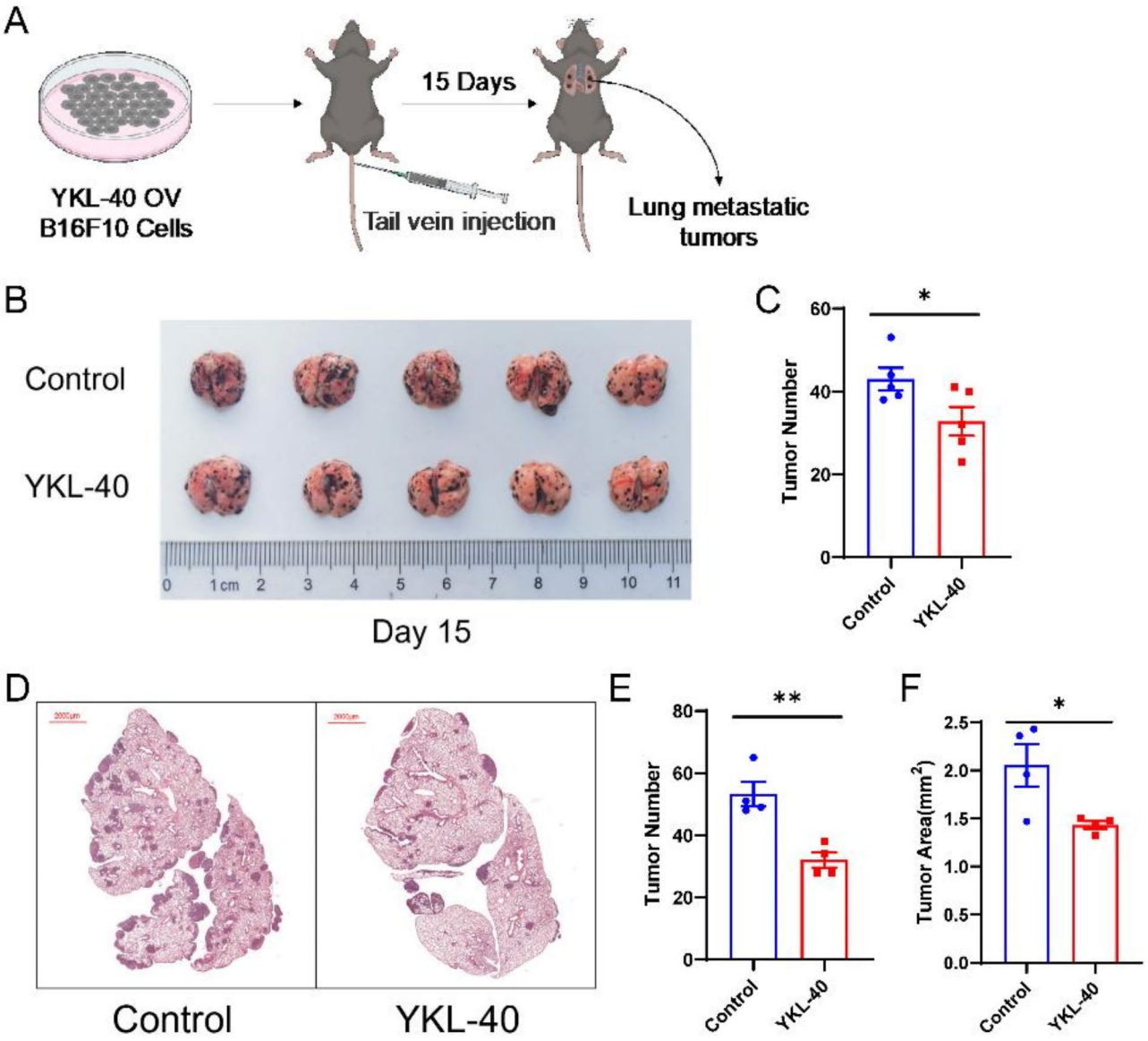


**Fig. 4**. YKL-40 inhibits tumor metastasis of melanoma in vivo. (**A**) Schematic of pulmonary metastasis model of melanoma in male C57BL/6 mice established via tail vein injection with B16F10 cells transfected with either blank vector or YKL-40 overexpression vector. (**B**) Images of lungs with melanoma taken on the 15th day after the model was established. (**C**) Histograms of tumor nodule numbers in the lung (bars, SEM; t-test; $^{*}P < 0.05$; $n = 5$). (**D**) H&E staining of lung tissue with metastatic melanoma. (**E** and **F**) Histograms of tumor numbers and area determined by H&E staining (bars, SEM; t-test; $^{*}P < 0.05$; $^{**}P < 0.01$; $n = 4$). YKL-40, chitinase 3 like 1.

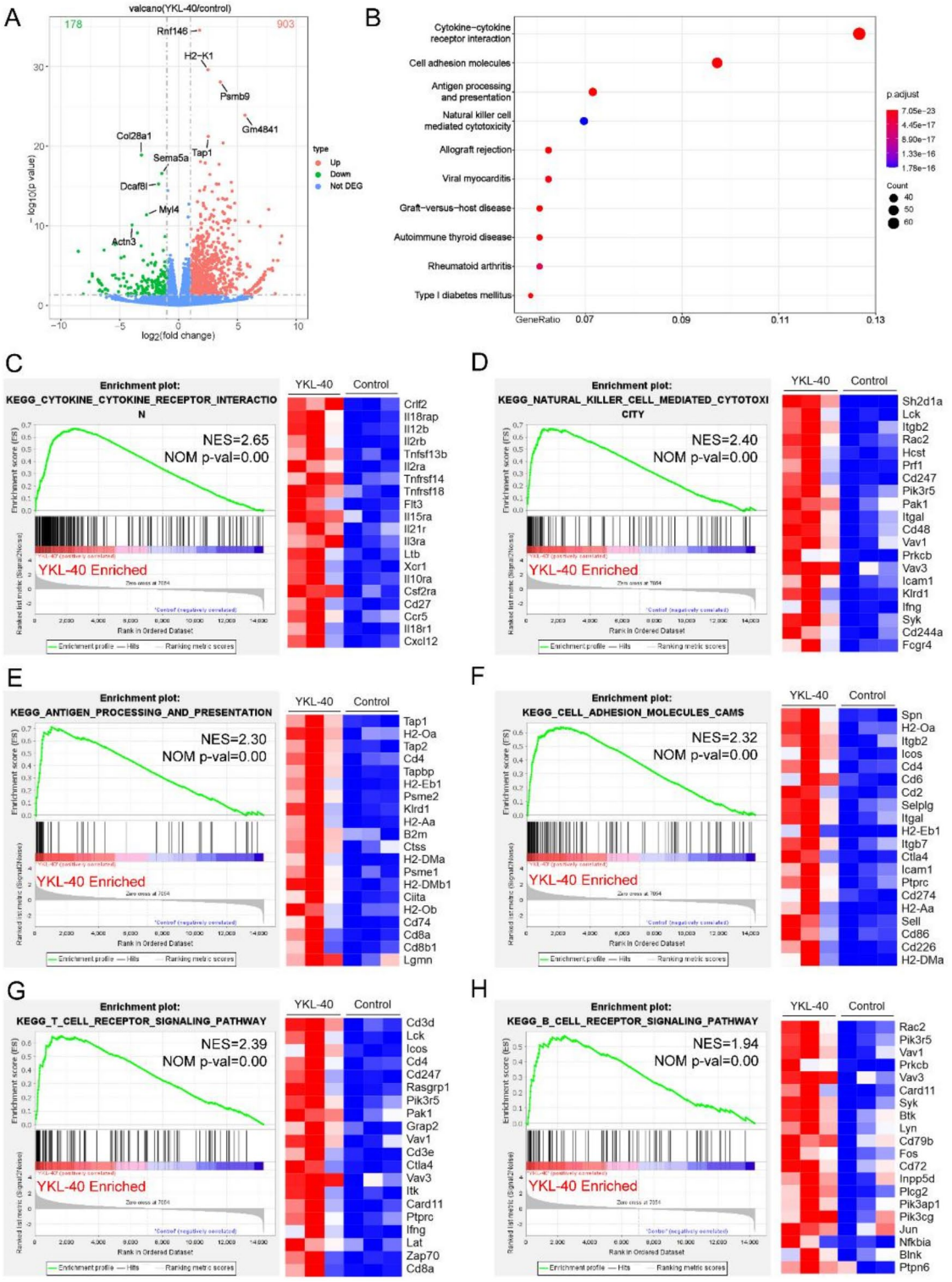


**Fig. 5**. Changes in YKL-40 expression cause changes in multiple genes and signaling pathways. (**A**) Volcano plot of differential mRNA expression determined using RNA-sequencing techniques. (**B**) Scatter plot of differential gene Kyoto Encyclopedia of Genes and Genomes enrichment[55]. (**C**–**H**) Selective hallmark gene sets showing the effects of YKL-40 were generated using the gene set enrichment analysis tool kit. Heat map showing the RNA expression levels (relative expression ratio compared with control) of differentially expressed genes were included in related gene set. YKL-40, chitinase 3 like 1.

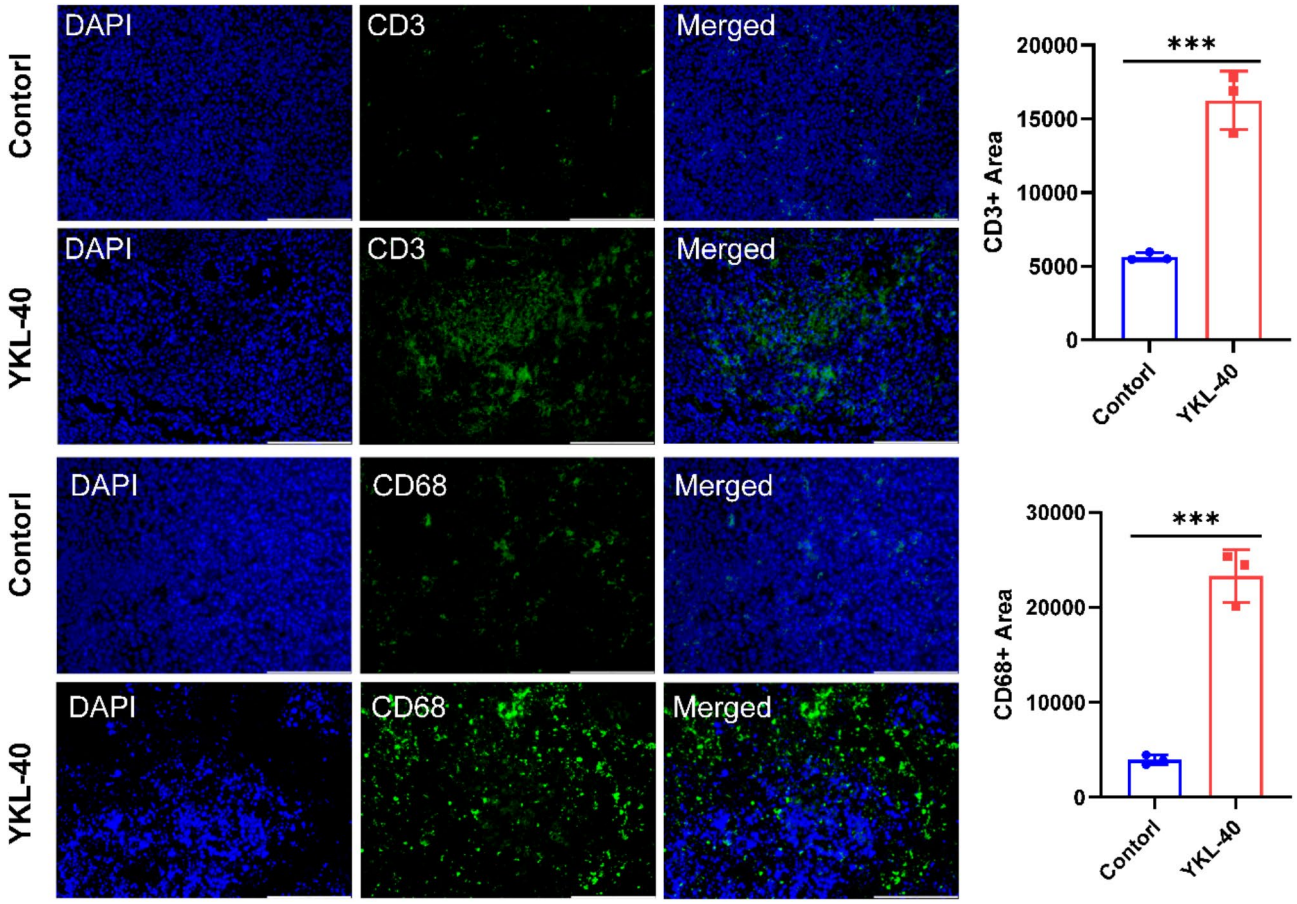


**Fig. 6**. YKL-40 overexpression enhances CD3 + and CD68 + immune cell infiltration in melanoma tumors. Immunohistochemical analysis of CD3+ (T cells) and CD68+ (macrophages) immune cell infiltration in melanoma tumors from control and YKL-40-overexpressing tumors. DAPI (blue) was used to stain cell nuclei. (bars, SD; t-test; $^{***}P < 0.001$; $n = 3$; Scale bar represents 50 μm).

in which significant enrichment of cytokine-cytokine receptor interaction and cell adhesion molecules was observed Fig. 5B). GSEA further highlighted the enrichment of cytokine interactions and immune cell activation pathways in the YKL-40 overexpression group Fig. 5C–H). T-cell activation-related genes, including Vav1, CD4, lfng and CD247, were significantly upregulated after YKL-40 overexpression. A group of genes responsible for B-cell receptor signaling and cell adhesion were also upregulated Fig. 5H). Consistent with the RNA-Seq results, the immunofluorescence staining demonstrates a significant increase in the infiltration of CD3 + T cells and CD68 + macrophages in melanoma tumors overexpressing YKL-40 compared to control tumors Fig. 6). Quantitative analysis of the CD3 + and CD68 + cell areas confirms this observation, with both cell types showing a statistically significant increase in the YKL-40 overexpressing group. Collectively, these findings suggested that YKL-40 overexpression in melanoma cells enhanced immune cell infiltration, potentially inhibiting tumor proliferation and invasion.

## Discussion

YKL-40 is recognized as a serum biomarker, and its levels are elevated in the serum and tissues of numerous solid tumors[30]. In melanoma, elevated plasma YKL-40 concentrations are associated with increased patient mortality[15,31,32]. Typically produced by immune cells, such as macrophages and neutrophils, YKL-40 acts as a growth factor for both vascular endothelial and cancer cells. Its expression is induced by a variety of cytokines, serving a pivotal role in inflammation-associated neoplastic transformations[20]. The present analysis revealed that YKL-40 expression within melanoma tumor tissues was markedly lower than that in normal skin tissues, suggesting disparate roles for YKL-40 originating from tumor cells compared with that from immune cells. This necessitates further investigation into the specific contributions of YKL-40 in tumor cells. In the present study, the biological effects of YKL-40 in the occurrence of melanoma were clarified. In vitro experiment results indicated that the proliferation, growth, migration and invasion of melanoma cells were inhibited after YKL-40 overexpression. In vivo animal experiments demonstrated that after injection of YKL-40-overexpressing B16F10 cells, tumor growth was slower in tumor-bearing mice and the ability of tumor cells to metastasize to the lungs was also reduced.

YKL-40 expression is pivotal in modulating the expression profile of receptors located on the cell membrane of melanoma cells. This includes receptors involved in cytokine signaling, antigen presentation and cell adhesion (Fig. 5). Scientific investigations have revealed that perturbations in cytokine levels among patients with melanoma can exert an influence on disease progression, therapeutic response and overall disease prognosis[33,34]. The differential effects of YKL-40 may be attributed to its distinct roles in systemic circulation and within the tumor microenvironment. In the serum, elevated YKL-40 levels have been associated with a poor prognosis, potentially due to its involvement in systemic inflammation and immune suppression[35]. This aligns with findings from other cancers where YKL-40 has been shown to contribute to an immunosuppressive environment[36]. Conversely, within the tumor microenvironment, YKL-40 may play a dual role. On one hand, it can inhibit tumor cell growth, and on the other hand, it can activate the immune system, promoting an antitumor immune response by enhancing immune cell infiltration and activation. Our RNA-seq analysis and immunofluorescence staining results support this hypothesis by demonstrating increased immune cell infiltration in YKL-40 overexpressing tumors.

Overexpression of YKL-40 upregulated genes associated with T-cell activation, including Vav1, CD4, lfng and CD247, as well as genes responsible for B-cell receptor signaling and cell adhesion. The high expression of interleukin receptors and TNF receptors indicates that a large number of immune cells exists in the tumor area, especially T cells[37]. Activation of tumor-associated antigen-specific $CD4^+$ T cells is critical for antitumor effects in vivo[38–40]. $CD4^+$ T cells can also interact directly with some tumor cells[41]. The expression of major histocompatibility complex (MHC) class II can be prompted in various cell types other than specialized antigen-presenting cells, such as tumor cells, when exposed to inflammatory cytokines, notably IFNγ, and through the activation of the transcriptional regulator class II transactivator. In humans, the expression of MHC class II in tumors is associated with favorable prognosis, improved tumor immunity and favorable reactions to immunotherapy[42,43].

Recent endeavors to determine the mechanisms propelling activation of $CD4^+$ T cells within tumors in humans have revealed that recognition of tumor cells by functionally distinct $CD4^+$ T cell clones from individuals with melanoma can occur directly with MHC II-positive melanoma cells, as well as indirectly through antigen-presenting cells bearing tumor antigens. Simultaneously, substantial MHC class II expression on human melanoma cells has been demonstrated to be linked to a heightened tumor mutational burden and an increased neo-antigen load that, in turn, could activate regulatory and exhausted $CD4^+$ T cells within the tumor microenvironment (TME). This implies that, in addition to advantageous immune effects, adverse immunosuppressive $CD4^+$ T cells may be induced in these patients[44]. CD247, also known as CD3ζ, is an important component of the T-cell receptor complex (TCR)[45], which involved in transmitting external antigenic stimulus signals and contributing to the activation of T cells[46]. CD247 is essential for the expression of cell surface TCR complexes, as surface levels of TCRs are reduced in $CD247^{-/-}$ mice[47], and the numbers of $CD4^+CD8^+$, $CD4^+CD8^-$ and $CD4^-CD8^+$ thymocytes are reduced[48,49]. CD247 expression was differentially downregulated in T cells from skin cancer[50]. A low level of CD3ζ expression was associated with a poor prognosis in patients with programmed death-ligand 1-negative melanoma, as determined by immunohistochemistry, and its low expression is associated with lower immune infiltration[51]. Therefore, investigating the specific mechanism underlying the regulation of T cell infiltration by YKL-40 holds significant importance in the context of anti-melanoma therapy and warrants further scientific examination.

Gene-targeted therapies have exhibited remarkable efficacy in melanoma treatment; however, the identification of effective targets remains a challenge[52–54]. The unique expression profile, impact on cell viability and regulatory effects on immune-related genes and pathways of YKL-40 make it a compelling candidate for anti-melanoma research. Given the role of YKL-40 in modulating immune responses within the TME, there is potential for combining YKL-40-targeted therapies with existing immunotherapies, such as immune checkpoint inhibitors. Enhancing YKL-40 expression or activity could increase T cell activation and infiltration, potentially synergizing with checkpoint inhibitors to overcome resistance and improve treatment outcomes. Clinical trials exploring combinations of YKL-40 modulation with immunotherapies could provide valuable insights into the therapeutic potential of such approaches. Further exploration of YKL-40 as a therapeutic target could provide novel avenues for melanoma treatment strategies.

In conclusion, YKL-40 presents an intriguing target in the treatment of melanoma, potentially improving prognosis, inhibiting tumor progression and enhancing the efficacy of immunotherapies. Further research into the mechanisms of action of YKL-40 in melanoma and the development of targeted therapeutic strategies will be crucial in translating these findings into clinical benefits for patients with melanoma.

## Data availability

The RNA-sequencing datasets generated and during the current study are available in the National Center for Biotechnology Information Gene Expression Omnibus database and can be accessed via the Gene Expression Omnibus series accession number GSE217590.

Received: 5 December 2024; Accepted: 28 February 2025
Published online: 03 March 2025

## References

1. Davis, L. E., Shalin, S. C. & Tackett, A. J. Current state of melanoma diagnosis and treatment. *Cancer Biol Ther.* **20**(11), 1366–1379 (2019).
2. Slominski, A., Tobin, D. J., Shibahara, S. & Wortsman, J. Melanin pigmentation in mammalian skin and its hormonal regulation. *Physiol. Rev.* **84**(4), 1155–1228 (2004).
3. Jenkins, R. W. & Fisher, D. E. Treatment of advanced melanoma in 2020 and beyond. *J. Invest. Dermatol.* **141**(1), 23–31 (2021).

4. Carlino, M. S., Larkin, J. & Long, G. V. Immune checkpoint inhibitors in melanoma. *Lancet* **398**(10304), 1002–1014 (2021).
5. Liu, D. et al. Evolution of delayed resistance to immunotherapy in a melanoma responder. *Nat. Med.* **27**(6), 985–992 (2021).
6. Marzagalli, M., Ebelt, N. D. & Manuel, E. R. Unraveling the crosstalk between melanoma and immune cells in the tumor microenvironment. *Semin. Cancer Biol.* **59**, 236–250 (2019).
7. Klobuch, S., Seijkens, T. T. P., Schumacher, T. N. & Haanen, J. B. A. G. Tumour-infiltrating lymphocyte therapy for patients with advanced-stage melanoma. *Nat. Rev. Clin. Oncol.* **21**(3), 173–184 (2024).
8. Chen, D. S. & Mellman, I. Elements of cancer immunity and the cancer-immune set point. *Nature* **541**(7637), 321–330 (2017).
9. Ribas, A. & Wolchok, J. D. Cancer immunotherapy using checkpoint blockade. *Science* **359**(6382), 1350–1355 (2018).
10. Fridman, W. H., Zitvogel, L., Sautes-Fridman, C. & Kroemer, G. The immune contexture in cancer prognosis and treatment. *Nat. Rev. Clin. Oncol.* **14**(12), 717–734 (2017).
11. Mantovani, A. & Sica, A. Macrophages, innate immunity and cancer: Balance, tolerance, and diversity. *Curr. Opin. Immunol.* **22**(2), 231–237 (2010).
12. Del Prete, A. et al. Dendritic cell subsets in cancer immunity and tumor antigen sensing. *Cell. Mol. Immunol.* **20**(5), 432–447 (2023).
13. Wolf, N. K., Kissiov, D. U. & Raulet, D. H. Roles of natural killer cells in immunity to cancer, and applications to immunotherapy. *Nat. Rev. Immunol.* **23**(2), 90–105 (2023).
14. Jacquelot, N., Duong, C. P. M., Belz, G. T. & Zitvogel, L. Targeting chemokines and chemokine receptors in melanoma and other cancers. *Front. Immunol.* **9**, 2480 (2018).
15. Schmidt, H. et al. Elevated serum level of YKL-40 is an independent prognostic factor for poor survival in patients with metastatic melanoma. *Cancer* **106**(5), 1130–1139 (2006).
16. Junker, N., Johansen, J. S., Andersen, C. B. & Kristjansen, P. E. Expression of YKL-40 by peritumoral macrophages in human small cell lung cancer. *Lung cancer (Amsterdam, Netherlands)* **48**(2), 223–231 (2005).
17. Jefri, M., Huang, Y. N., Huang, W. C., Tai, C. S. & Chen, W. L. YKL-40 regulated epithelial-mesenchymal transition and migration/invasion enhancement in non-small cell lung cancer. *BMC Cancer* **15**, 590 (2015).
18. Francescone, R. A. et al. Role of YKL-40 in the angiogenesis, radioresistance, and progression of glioblastoma. *J. Biol. Chem.* **286**(17), 15332–15343 (2011).
19. Schultz, N. A. & Johansen, J. S. YKL-40-A protein in the field of translational medicine: A role as a biomarker in cancer patients?. *Cancers (Basel)* **2**(3), 1453–1491 (2010).
20. Libreros, S. & Iragavarapu-Charyulu, V. YKL-40/CHI3L1 drives inflammation on the road of tumor progression. *J. Leukoc. Biol.* **98**(6), 931–936 (2015).
21. Hao, H., Chen, H., Xie, L. & Liu, H. YKL-40 promotes invasion and metastasis of bladder cancer by regulating epithelial mesenchymal transition. *Ann. Med.* **53**(1), 1170–1178 (2021).
22. Hao, H. et al. YKL-40 promotes the migration and invasion of prostate cancer cells by regulating epithelial mesenchymal transition. *Am. J. Transl. Res.* **9**(8), 3749–3757 (2017).
23. Li, L. L., Fan, J. T., Li, D. H. & Liu, Y. Effects of a small interfering RNA targeting YKL-40 gene on the proliferation and invasion of endometrial cancer HEC-1A cells. *Int. J. Gynecol. Cancer* **26**(7), 1190–1195 (2016).
24. Holst, C. B. et al. Perspective: Targeting VEGF-A and YKL-40 in glioblastoma - matter matters. *Cell Cycle* **20**(7), 702–715 (2021).
25. Kim, K. C. et al. Suppression of metastasis through inhibition of chitinase 3-like 1 expression by miR-125a-3p-mediated up-regulation of USF1. *Theranostics* **8**(16), 4409–4428 (2018).
26. Shao, R. et al. Anti-YKL-40 antibody and ionizing irradiation synergistically inhibit tumor vascularization and malignancy in glioblastoma. *Carcinogenesis* **35**(2), 373–382 (2014).
27. Kang, K. et al. Selection and characterization of YKL-40-targeting monoclonal antibodies from human synthetic fab phage display libraries. *Int. J. Mol. Sci.* **21**(17), 6354 (2020).
28. Salamon, J. et al. Antibody directed against human YKL-40 increases tumor volume in a human melanoma xenograft model in scid mice. *PLoS One* **9**(4), e95822 (2014).
29. Erturk, K., Tas, F., Serilmez, M., Bilgin, E. & Yasasever, V. Clinical significance of serum Ykl-40 (Chitinase-3-Like-1 Protein) as a biomarker in melanoma: An analysis of 112 Turkish patients. *Asian Pac. J. Cancer Prev.* **18**(5), 1383–1387 (2017).
30. Rusak, A., Jablonska, K. & Dziegiel, P. The role of YKL-40 in a cancerous process. *Postepy higieny i medycyny doswiadczalnej (Online).* **70**, 1286–1299 (2016).
31. Krogh, M. et al. Prognostic and predictive value of YKL-40 in stage IIB-III melanoma. *Melanoma Res.* **26**(4), 367–376 (2016).
32. Ismail, H. et al. Measured and genetically predicted plasma YKL-40 levels and melanoma mortality. *Eur. J. Cancer* **121**, 74–84 (2019).
33. Wang, X. et al. Serum cytokine profiles of melanoma patients and their association with tumor progression and metastasis. *J. Oncol.* **2021**, 6610769 (2021).
34. Koroknai, V., Szász, I. & Balázs, M. Gene expression changes in cytokine and chemokine receptors in association with melanoma liver metastasis. *Int. J. Mol. Sci.* **24**(10), 8901 (2023).
35. Taifour, T. et al. The tumor-derived cytokine Chi3l1 induces neutrophil extracellular traps that promote T cell exclusion in triple-negative breast cancer. *Immunity* **56**(12), 2755–2772 (2023).
36. Wang, Z. et al. YKL-40 derived from infiltrating macrophages cooperates with GDF15 to establish an immune suppressive microenvironment in gallbladder cancer. *Cancer Lett.* **563**, 216184 (2023).
37. Kalaora, S., Nagler, A., Wargo, J. A. & Samuels, Y. Mechanisms of immune activation and regulation: lessons from melanoma. *Nature Reviews Cancer.* **22**(4), 195–207 (2022).
38. Poncette, L., Chen, X., Lorenz, F. K. & Blankenstein, T. Effective NY-ESO-1-specific MHC II-restricted T cell receptors from antigen-negative hosts enhance tumor regression. *J. Clin. Invest.* **129**(1), 324–335 (2019).
39. Bos, R. & Sherman, L. A. CD4+ T-cell help in the tumor milieu is required for recruitment and cytolytic function of CD8+ T lymphocytes. *Cancer Res.* **70**(21), 8368–8377 (2010).
40. Quezada, S. A. et al. Tumor-reactive CD4(+) T cells develop cytotoxic activity and eradicate large established melanoma after transfer into lymphopenic hosts. *J. Exp. Med.* **207**(3), 637–650 (2010).
41. Speiser, D. E., Chijioke, O., Schaeuble, K. & Münz, C. CD4(+) T cells in cancer. *Nat. Cancer* **4**(3), 317–329 (2023).
42. Seliger, B., Kloor, M. & Ferrone, S. HLA class II antigen-processing pathway in tumors: Molecular defects and clinical relevance. *Oncoimmunology* **6**(2), e1171447 (2017).
43. Axelrod, M. L., Cook, R. S., Johnson, D. B. & Balko, J. M. Biological consequences of MHC-II expression by tumor cells in cancer. *Clin. Cancer Res.* **25**(8), 2392–2402 (2019).
44. Oliveira, G. et al. Landscape of helper and regulatory antitumour CD4(+) T cells in melanoma. *Nature* **605**(7910), 532–538 (2022).
45. Weissman, A. M. et al. Molecular cloning and chromosomal localization of the human T-cell receptor zeta chain: Distinction from the molecular CD3 complex. *Proc. Natl. Acad. Sci. USA* **85**(24), 9709–9713 (1988).
46. Dexiu, C., Xianying, L., Yingchun, H. & Jiafu, L. Advances in CD247. *Scand. J. Immunol.* **96**(1), e13170 (2022).
47. Malissen, M. et al. T cell development in mice lacking the CD3-zeta/eta gene. *Embo J.* **12**(11), 4347–4355 (1993).
48. Love, P. E. et al. T cell development in mice that lack the zeta chain of the T cell antigen receptor complex. *Science* **261**(5123), 918–921 (1993).
49. Liu, C. P. et al. Abnormal T cell development in CD3-zeta-/- mutant mice and identification of a novel T cell population in the intestine. *Embo J.* **12**(12), 4863–4875 (1993).

50. Alaibac, M., Pigozzi, B., Saponeri, A., Belloni-Fortina, A. & Peserico, A. Absent or low expression of T-cell receptor zeta-chain in T cells infiltrating human pathological skin conditions. *Arch. Dermatol. Res.* **294**(8), 380–382 (2002).
51. Zhang, Z. et al. CD3ζ as a novel predictive biomarker of PD-1 inhibitor resistance in melanoma. *Mol. Cell. Probes.* **72**, 101925 (2023).
52. Teixido, C., Castillo, P., Martinez-Vila, C., Arance, A. & Alos, L. Molecular markers and targets in melanoma. *Cells* **10**(9), 2320 (2021).
53. Lazaroff, J. & Bolotin, D. Targeted therapy and immunotherapy in melanoma. *Dermatol. Clin.* **41**(1), 65–77 (2023).
54. Guo, W., Wang, H. & Li, C. Signal pathways of melanoma and targeted therapy. *Signal Transduct. Target Ther.* **6**(1), 424 (2021).
55. Kanehisa, M., Furumichi, M., Sato, Y., Matsuura, Y. & Ishiguro-Watanabe, M. KEGG: Biological systems database as a model of the real world. *Nucleic Acids Res.* **53**(D1), D672–D677 (2025).

## Author contributions
HZ and XZ contributed equally to designing the study and obtaining the data. MS, YH and KL carried out the animal experiments. YiW, WY and YuW conceived/designed the experiments. HW, SS and BY established the cell lines. ZG, MQ and GW helped interpret the data and contributed to the critical conception of the study. HZ, MS and YuW confirmed the authenticity of all the raw data, wrote and revised the manuscript. All authors contributed to the article, read and approved the final manuscript.

## Funding
The present study was supported by the Shandong Provincial Natural Science Foundation (grant nos. ZR2020MH146 and ZR2020QH084).

## Declarations

## Competing interests
The authors declare no competing interests.

## Ethics approval and consent to participate
The animal experiments were approved by the Ethics Committee of Weifang No.2 People's Hospital (approval no. 2024LAC019; Weifang, China).

## Additional information
**Supplementary Information** The online version contains supplementary material available at https://doi.org/10.1038/s41598-025-92522-7.

**Correspondence** and requests for materials should be addressed to W.Y. or Y.W.